Sensor Fusion-based Parameterized Curve-driven Modeling for Digital Twin of Reconfigurable Soft Robot*

Zhongyuan Liao[1], Wanzhen Wei[2], Leihan Zhang[2] and Yi Cai[3]

***Abstract*— Soft robotics, driven by material and design advancements, presents challenges for visualization and simulation due to its complex deformations. This paper proposes a digital twin (DT) system for reconfigurable soft robots in augmented reality (AR) environments. Leveraging parameterized curve-driven methods, the system enables dynamic modification of digital twins, accurately representing deformations. Three primary deformation patterns are identified, and sensor fusion captures real-time structural changes. Implemented within an AR environment, the system allows immersive inspection and simulation of soft robots. A case study validates its effectiveness.**

***Keywords*: Digital Twin, Sensor Fusion, Augmented Reality, Reconfigurable Soft Robot, Parameterized curve**

I. INTRODUCTION

Soft robotics represents a burgeoning domain characterized by the utilization of pliable materials, where the locomotion of such robots is predominantly achieved through the inherent elastic deformation of their structural makeup. Attributable to their intrinsic properties, marked flexibility, substantial compliance, adaptability, and enhanced safety during human-robot interactions, soft robots have garnered escalating scholarly interest. They exhibit promising applicative prospects across various sectors, including medical instrumentation, wearable technology, and industrial systems [1].

The paradigm of reconfigurability has emerged as a salient trend within contemporary industrial processes [2], advocating for the segmentation of large and intricate products or systems into smaller, modular, and manageable units. Diverging from their fixed-morphology counterparts, reconfigurable soft robots (RSR) possess the innate ability to conform to diverse environmental contexts and task-specific requirements through the reorganization of their modular components. This capability facilitates advanced functionalities, encompassing self-assembly, self-repair, and autonomous actuation. RSR confers distinct advantages, including streamlined maintenance, customizable configurations, scalability for mass production, and enhanced reusability. Current research trajectories in the field of RSR are chiefly concentrated on the development of modular unit design, simulation methodologies, manufacturing techniques, connective mechanics, sensor integration, and control strategies. A spectrum of reconfigurable soft robot prototypes has been realized, ranging from soft modular constructs akin to LEGO [3], chiral-lattice structures adaptable for locomotion [4], spherical RSR [5], flexible robotic arms [6], to origami-inspired RSR configurations [7]. Despite the proliferation of exploratory endeavors in the realm of RSR, the establishment of systematic theoretical frameworks for their design and operationalization remains nascent. Predominantly, extant designs have been directed toward practical applications with a paucity of advanced visualization and simulation techniques.

Digital twins, virtual avatars of physical entities, are an avant-garde technology within contemporary industrial landscapes, offering two primary capabilities: visualization and simulation in practical application[8], [9]. Nonetheless, the application of these functionalities to soft robotics is problematic due to their intrinsic and pronounced deformability. Yang et al. [10] proposed a virtual work-based static model to describe the mechanics of continuum robots with rod-driven structures, accounting for geometric constraints of the drive rods. To precisely capture the complex deformations characteristic of soft robots, the integration of bending sensors has proven indispensable. These sensors facilitate the acquisition of real-time deformation data, thereby enhancing the fidelity of the robot's digital counterpart. Koivikko et al. [11] devised stretchable pneumatic strain gauges tailored for soft robotic applications, whereas Wang et al. [12] developed a highly elastic hydrogel sensor that adeptly monitors multi-modal interactions, including bending, twisting, and force detection, with remarkable sensitivity in soft robotic fingers. Furthermore, White et al.[13] introduced a multi-element strain gauge module for soft sensory skins, equipped with a trio of resistive gauges to amass comprehensive geometric data. In a synergistic fusion with augmented reality (AR), DT can offer real-time informational overlays, facilitating a more naturalistic and intuitive interface for human-robot interaction, thus forging an immersive experiential nexus within the realm of RSR. Drawing upon sensorized soft bending robot, Borges et al. [14] put forth a conceptual framework for shape reconstruction within the context of extended reality. This integration of bending sensors within a DT enables the generation of a real-time portrayal of soft robots. However, most current representations are rudimentary proxies—such as curves or planes—that fall short of mirroring the true three-dimensional deformed structures. Concerning the simulation aspect, research efforts directed at configuration simulation are scarce, and even more so when considering the confluence with human operators. Presently, the RSR domain is bereft of a robust and accurate visualization and simulation platform, an instrumental tool for advancing the field.

Here, we introduce an innovative methodology for the synthesis of a digital twin tailored to a reconfigurable soft robot through the implementation of augmented reality (AR) technology. Our proposed system facilitates the instantaneous and uninterrupted depiction of the robot's deformation within an AR milieu, empowering users to adjust the configuration of the soft modular components. Additionally, it provides the capability to simulate these alterations in AR to accommodate a diverse array of functional task demands. The structure of the rest paper is arranged as follows: Section 2 delineates the DT framework alongside the pertinent theoretical underpinnings expounded in Section 3. Section 4 delineates a practical case study, culminating in Section 5, which synthesizes key insights and noteworthy conclusions derived from our study.

*This work was supported by HKUST(GZ)

[1]Zhongyuan Liao is with Ph.D. candidate of Division of Emerging Interdisciplinary Areas (EMIA), Academy of Interdisciplinary Studies, The Hong Kong University of Science and Technology, Hong Kong SAR, China zliaoao@connect.ust.hk

[2]Wanzhen Wei and Leihan Zhang are with the Smart Manufacturing Thrust, Systems Hub, The Hong Kong University of Science and Technology (Guangzhou), Guangzhou, China

[3]Yi Cai is with the faculty of Smart Manufacturing Thrust, Systems Hub, The Hong Kong University of Science and Technology (Guangzhou), Guangzhou, China. Corresponding author, yicai@hkust-gz.edu.cn

II. The Frameworks of Digital Twin System

The framework of the DT system for RSR is designed to offer a user-friendly platform that facilitates seamless visualization and interaction. This allows users to accurately perceive the deformation of RSR, as well as simulate its configuration with intuitive interaction. The framework consists of three primary components: modular design and fabrication, parametric curve-based visualization and control, and sensor fusion, as depicted in Fig.1.

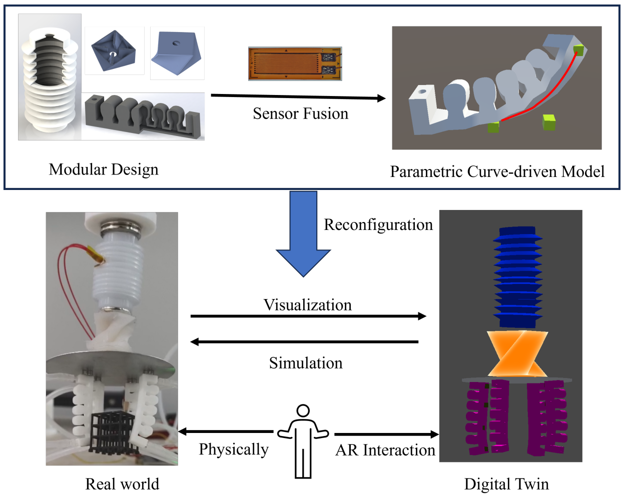

Fig. 1. The framework of the AR-enhanced digital twin system for reconfigurable soft robots.

The project utilizes a modular design for reconfigurable robots, allowing easy adaptation to tasks through interchangeable modules enabling stretching, bending, and twisting. Parametric curve-based visualization within an AR environment facilitates continuous deformation exploration, enhancing user interaction by simulating various configurations virtually. Sensor fusion, employing low-cost strain gauge sensors, reconstructs real-time deformation, mapping it to parametric curves for accurate real-world movement simulation in the AR environment. This approach provides precise control for the DT robots, ensuring seamless and accurate movement in response to environmental changes or user input.

AR allows for the seamless embedding of digital elements into the real world, enhancing the user's perception. In this context, the DT system operates alongside the real environment, utilizing AR to simulate various configurations within the user's actual surroundings. This integration enables a more immersive experience, where the digital and physical worlds interact seamlessly.

III. Methodology

A. Modular Design and Fabrication for Three Primary Patterns

The tripartite modular design is derived from the fundamental motion patterns observed in conventional soft robot designs. This design approach employs additive manufacturing and molding techniques to effectively fabricate the final product. The stretch module is inspired by the folding zones of Chinese lanterns, allowing for longitudinal stretching. The twisting module incorporates a propeller-like structure consisting of two parallel square plates connected by four twisted blades. By directing airflow through the chamber, an unbalanced force distribution is created, resulting in twisting deformation. Conversely, the bending module utilizes a chamber with a wider upper section and a narrower lower section to induce bending deformation. These three modules, as illustrated in Figure 2, collectively contribute to the overall functionality of the tripartite modular design. More design and fabrication details can be referred to the previous works [15], [16]. For convenience assembly and disassembly, the magnet connection is utilized.

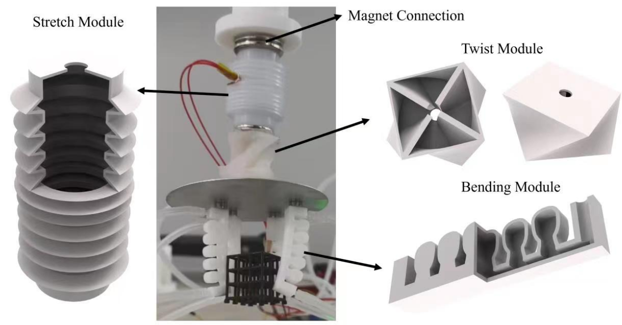

Fig. 2. The structure design of three basic soft modules.

B. Parametric Curve-based Visualization and Control

The concept of parametric curve-based visualization and control has been utilized in this approach, with a specific emphasis on the Bezier curve model. This model consists of n control points and plays a crucial role in determining the deformation patterns of the robot. The curve is comprised of several bones that are distributed along its points, which define the location and orientation of the robot's modules.

The bone functionality in Blender serves as a crucial component in the rigging and animation process. It represents a joint or segment within a skeletal structure and allows for the manipulation and control of 3D models. By adding, editing, and positioning bones, complex armatures can be created to accurately deform and animate characters or objects. This capability is particularly useful when working with soft robotic modules, where the bone framework can be utilized to simulate the flexible and dynamic behavior of these modules.

Fig. 3 illustrates the weight painting process applied to a bone, revealing its impact on the deformation of the soft robot module. This weight painting technique involves assigning distinct weights to each vertex of the module, taking into consideration the distance. The closer the vertex is to the bone, the higher the assigned weight, which determines the extent to which the movement of the associated bone affects that particular vertex.

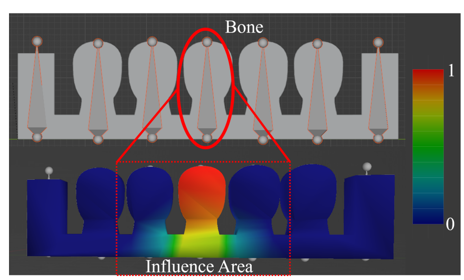

Fig. 3. Weight paint of a bone on a soft robot module. The color-coded weight distribution determines the influence of the bone on the deformation of the module.

The bone-based model can be subsequently exported to Unity for further development. By using Blender's bone system, intricate skeletal structures can be constructed to facilitate continuous deformations of soft robots. This enables the user to establish precise control over the model's movements and expressions. Once exported to Unity, the bone structure is attached to the control point of the parametric Bezier curve. By manipulating the control points, the parameterized curve is altered, and the corresponding bones on the curve are also modified, ultimately resulting in continuous deformation of the modules. The seamless integration of bone functionality between Blender and Unity enhances the overall workflow and facilitates the creation of visually compelling and interactive 3D experiences.

The equation for the Bezier curve $B(t)$ is:

$$B(t) = \sum_{i=0}^{n} P_i B_i^n(t) \tag{1}$$

where P_i are the position of control points, n is the degree of the curve, and $B_i^n(t)$ are the Bernstein basis polynomials defined as:

$$B_i^n(t) = \binom{n}{i}(1-t)^{n-i}t^i \tag{2}$$

where the parameter t is in the range [0,1].

The tangent vector at any given point on the curve is given by its first derivative $B'(t)$.

$$B'(t) = n\sum_{i=0}^{n-1}(P_{i+1} - P_i)B_i^{n-1}(t) \tag{3}$$

where P_i are the control points, n is the degree of the curve, and $B_i^{n-1}(t)$ are the Bernstein basis polynomials defined as:

$$B_i^{n-1}(t) = \binom{n-1}{i}(1-t)^{n-1-i}t^i \tag{4}$$

Here, a variable $PB = [PB_0, PB_1, ..., PB_i, ..., PB_m]$ is utilized to represent the location of the chamber's bone, where m is the number of the bones, each PB_i denotes the position of a bone on the Bezier curve, represented as:

$$PB_i = B(t), t = i/m \tag{5}$$

For simplicity, the bones are arranged in equal distance. By adjusting this variable PB, it is possible to drive the corresponding part of the robot to deform as required, thereby enabling a high degree of control over the robot's configuration and movement patterns.

For each bone on the curve, they are set to be vertical to the curve. The normal vector is the vector perpendicular to this tangent vector. In the 2D case, the normal vector $N(t)$ can be easily calculated by rotating the tangent vector by 90 degrees. Specifically, if $B'(t) = (x, y)$, then $N(t) = (-y, x)$ or $N(t) = (y, -x)$, depending on the orientation. In the 3D case, there is no unique normal vector. For 3D curves, normal vectors are infinite in the normal plane. Thus, a unique normal direction is defined by the tangent direction, which is a 90° rotation around the x-axis. It is represented as:

$$N = R \cdot B'(t) \tag{6}$$

where R is the rotation matrix. More motion transformation can be referred to [17]. In the case of 3D curves, the determined tangent line possesses two distinct directions. In order to maintain a continuous deformation, it is necessary to impose constraints on tangent directions, ensuring that the crossing angle between adjacent tangent directions remains below 90°.

Figure 4 illustrates the deformation that arises when altering the positions of control points. This representation showcases the Bezier curve, a space curve determined by the control points, visually represented as the red line. Moreover, the control points are visually denoted by green cubes. Additionally, the blue arrows serve to indicate the orientation of the bone, which is positioned orthogonally to the Bezier curve. The cubes, which represent the positions of the control points, can be manipulated, thereby modifying the deformation of the soft robot module. By displacing the cube in a specific direction, the module can be stretched. Similarly, bending can be achieved by moving the cube within the plane, while twisting can be accomplished by displacing the cube in three-dimensional space.

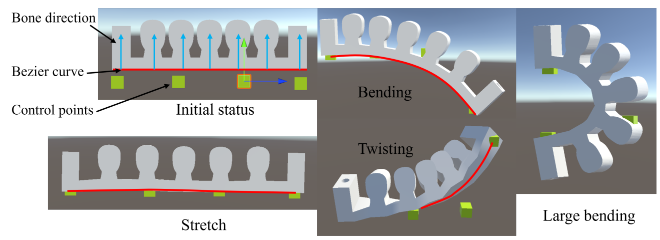

Fig. 4. The continuous deformation with different positions of control points (the green cubes).

C. Sensor Fusion

A succinct sensor fusion approach is introduced in order to accurately measure the actual deformation of various types of modules in their natural environment. This method relies solely on the utilization of a strain gauge (SG), a simple yet effective sensor, see Fig.5. The operational principle of the resistance strain gauge is predicated on the strain phenomenon, wherein the resistance value of a conductor or semiconductor material alters proportionally with its mechanical deformation under external forces, commonly referred to as the "strain effect". By affixing the strain gauge to the material to be measured, it flexes in accordance with the strain experienced by the material, causing the internal metal foil to also bend correspondingly.

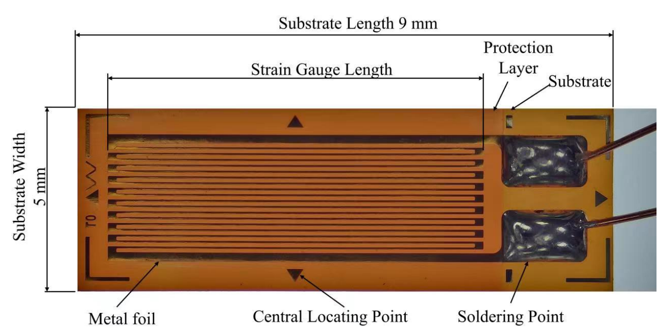

Fig. 5. The sensor structure of resistance strain gauge.

1) Bending Measurement: In the theory of strain gauge (SG) measurement, the relationship between strain and the corresponding change in resistance can be expressed using the equation:

$$\varepsilon = \frac{\Delta R}{R} \cdot \frac{1}{S} \tag{7}$$

Here, ε represents the strain, ΔR represents the change in resistance, R represents the initial resistance, and S represents the gauge factor. The gauge factor, denoted as S, is a characteristic parameter of the strain gauge that indicates the ratio of the relative change in resistance to the applied strain.

To incorporate bending measurement using a strain gauge, the equation can be modified to account for the bending strain. Bending strain is a result of the curvature or deflection of the material under external forces. The modified equation for bending strain can be expressed as:

$$\varepsilon_b = \frac{\Delta R_b}{R} \cdot \frac{1}{S_b} \tag{8}$$

where ε_b represents the bending strain, ΔR_b denotes the change in resistance due to bending, R signifies the initial resistance, and S_b represents the gauge factor for bending strain.

When both bending and axial strains are present, the total strain can be calculated as the sum of the bending strain (ε_b) and the axial strain (ε_a):

$$\varepsilon_{\text{total}} = \varepsilon_b + \varepsilon_a \tag{9}$$

Similarly, the total change in resistance (ΔR_{total}) can be obtained by adding the change in resistance due to bending (ΔR_b) and the change in resistance due to axial strain (ΔR_a):

$$\Delta R_{\text{total}} = \Delta R_b + \Delta R_a \tag{10}$$

When the axial strain is imperceptible, it becomes possible to ascertain the change in resistance, thereby enabling the assessment of the effect of bending when the object is connected to the flexible module. With the sensor bending, the corresponding resistance value changed in Fig.6.

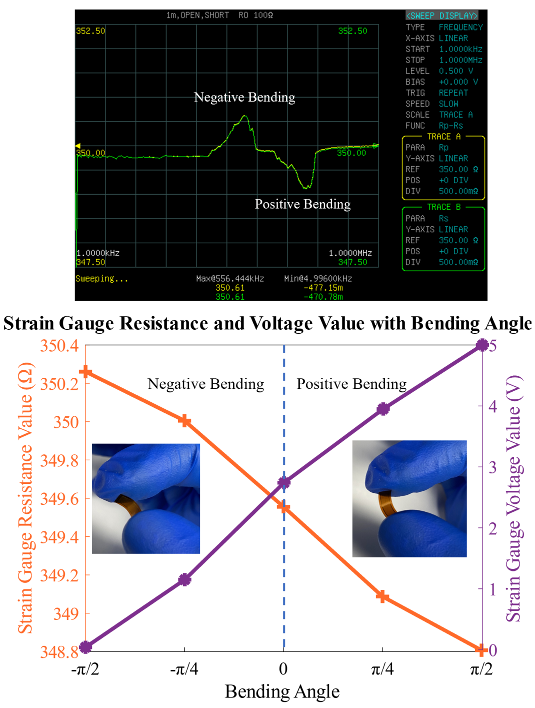

Fig. 6. The upper figure represents the measurement curve using the LCR meter, while the lower figure illustrates the fluctuation of the strain gauge resistance value and the voltage output value in correlation with varying bending angles.

The strain gauge measurement theory provides a robust framework for accurately assessing deformation and strain experienced by various modules in real-world scenarios. In practical applications, the change in measured resistance is converted into a voltage signal V using a Wheatstone bridge circuit, as depicted in Fig.7. This voltage signal can then be amplified and processed for further analysis and interpretation. Different deployment layouts are utilized for the various modules. In the bending module, the sensor is positioned flatly on the bottom face, allowing it to directly reflect the bending angle when the module deforms. In the stretch module, the strain gauge is placed on the gap between folds, enabling it to register changes in length. In the twisting module, the strain gauge is positioned on the side face to correspondingly register twists. By analyzing the output voltage of the strain gauge, the true deformation of the different modules can be easily determined.

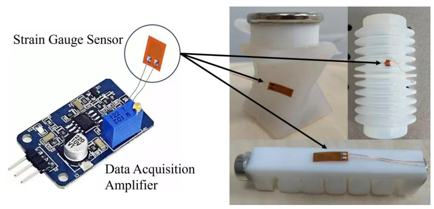

Fig. 7. The sensor deployment of three modules with the data collection module.

2) Calibration: The data collected from sensors requires processing and analysis. The first step involves calibration to establish a correlation between the sensed values and the position of the control point. Within each module, specific deformation statuses are selected as points along the known trajectory. These points are used to construct a continuous trajectory for each control point using a Bezier curve. This is achieved through reverse calculation. Let $PT = [PT_0, PT_1, PT_2, ..., PT_n]$ represent the set of known trajectory points, where n is the total number of known trajectory points.

The goal is to determine the control points $C = [C_0, C_1, C_2, ..., C_n]$ that enable the generation of a Bezier curve passing through the given trajectory points, with $PT_0 = C_0$ and $PT_n = C_n$.

The control points C are calculated using the equation:

$$C_i = \binom{n}{i} \cdot PT_i \tag{11}$$

where C_i represents the i-th control point, PT_i denotes the i-th known trajectory point, and $\binom{n}{i}$ represents the binomial coefficient.

Once the control points C are determined, the original Bezier curve formula PT is used to compute the fitted trajectory points within the given parameter T. The formula is as follows:

$$PT(T) = \sum_{i=0}^{n} \binom{n}{i} \cdot (1-T)^{n-i} \cdot T^i \cdot C_i \tag{12}$$

The sensor fusion method incorporates a fitting function to establish the relationship between the position of the control points (TC) and a voltage signal (V), which can be expressed by the equation:

$$T = f(V) = mV + c, T \in [0,1] \tag{13}$$

In this work, a linear mapping is utilized, where m represents the slope and c represents the y-intercept of the line. By mapping the parameter V to parameter T, a smooth trajectory can be generated, with each input V corresponding to a specific deformation. The fitted trajectory points obtained through this process serve as a representation of a smooth trajectory passing through the given set of trajectory points. This fitting function enables the integration of sensors with the digital twin system, allowing for accurate visualization of the same deformation observed in the real world. Fig.8 illustrates a comparison between the observed physical deformations in the soft modules and the analogous deformations within their virtual equivalents as part of a DT framework. This system enables users to engage in an interactive manipulation of the soft module through AR interfaces, thereby allowing for the pre-emptive simulation of functional behaviors prior to actual operation. Such a feature facilitates the exploration and assessment of diverse configurations across a spectrum of potential applications.

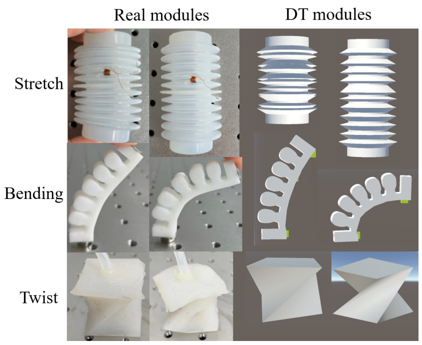

Fig. 8. The deformation comparison between the real soft modules and their digital twin.

IV. Case Study

This section elucidates the utilization of soft modules in configuring diverse arrangements to fulfill various functionalities. Illustrated in Fig. 9, are several assemblies of configurations achieved through soft modules, capable of executing walking, crawling, and gripping operations.

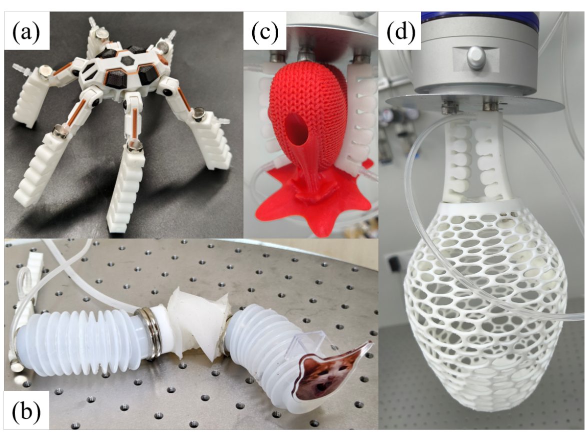

Fig. 9. The varied configurations facilitated by soft modules encompass: a) walking spider, b) crawling robot, c) external gripper, and d) internal gripper.

Subsequently, we provide a detailed discussion on the construction of a gripper utilizing three foundational modules, as illustrated in Fig. 10. The gripper is designed to perform intricate movements involving stretching, twisting, and bending. When the gripper undergoes deformation from pressure, a sensor collects the deformation data and transmits it to the HoloLens 2. Consequently, the AR-based DT system adjusts to accurately represent the actual deformation. Furthermore, the user can manipulate the modules, reposition them, change their posture, or add/drop modules within the DT system via AR interaction. This enables the user to simulate various configurations to determine the optimal setup for the soft robot, leading to enhanced efficiency and improved development iteration. The use of magnets to connect the modules facilitates easy reconfiguration by the user in the physical world. The case study demonstrates that the proposed DT system can facilitate the reconfiguration of soft modules in both real-world and DT systems, and enables the in-situ visualization of soft deformation within an immersive augmented reality environment, thereby showcasing the effectiveness and superiority of the proposed DT system.

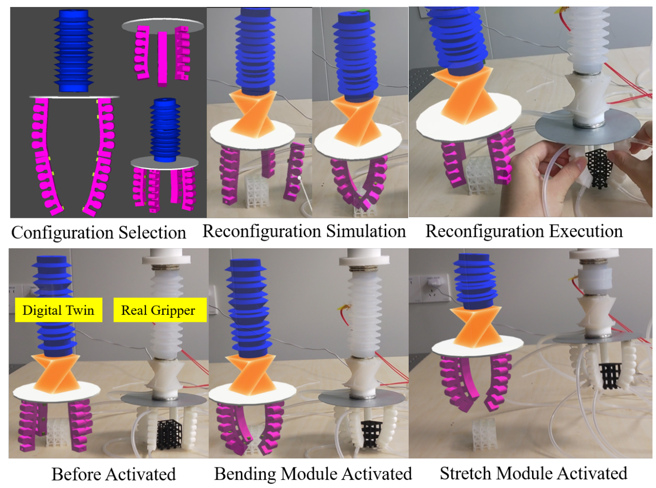

Fig. 10. The procedure of manipulation by DT-enable RSR gripper (in the real vision of HoloLens 2).

V. Conclusion

This paper introduces a novel framework for developing a digital twin (DT) system for reconfigurable soft robots within an augmented reality (AR) setting. The framework involves the integration of armature-based techniques and bending sensors to accurately capture the robots' deformation. The approach utilizes armature-based techniques to modify and reconstruct the digital twin of the soft deformation in the AR environment, facilitating smooth transitions between different deformations. The study identifies three fundamental types of deformation patterns - stretching, bending, and twisting - and corresponding visualization patterns to accurately represent these basic deformations. The sensor fusion method is introduced to map the relationship between sensor data and deformation, enabling more precise visualization and simulation within the AR environment. Finally, a case study is conducted, which successfully achieves reconfiguration in both the real world and the DT, as well as in-situ smooth visualization in the AR environment, demonstrating the effectiveness of the proposed method. Future research may explore extending this framework to control, manipulation, and human-robot interaction in various scenarios.

References

[1] N. El-Atab, R. B. Mishra, F. Al-Modaf, L. Joharji, A. A. Alsharif, H. Alamoudi, M. Diaz, N. Qaiser, and M. M. Hussain, "Soft actuators for soft robotic applications: a review," *Advanced Intelligent Systems*, vol. 2, no. 10, p. 2000128, 2020.

[2] A. Brunete, A. Ranganath, S. Segovia, J. P. de Frutos, M. Hernando, and E. Gambao, "Current trends in reconfigurable modular robots design," *International Journal of Advanced Robotic Systems*, vol. 14, no. 3, p. 1729881417710457, 2017.

[3] J.-Y. Lee, J. Eom, W.-Y. Choi, and K.-J. Cho, "Soft lego: bottom-up design platform for soft robotics," in *2018 IEEE/RSJ International Conference on Intelligent Robots and Systems (IROS)*. IEEE, 2018, pp. 7513–7520.

[4] D. Wang, B. Zhao, X. Li, L. Dong, M. Zhang, J. Zou, and G. Gu, "Dexterous electrical-driven soft robots with reconfigurable chiral-lattice foot design," *Nature Communications*, vol. 14, no. 1, p. 5067, 2023.

[5] C. Freeman, M. Maynard, and V. Vikas, "Topology and morphology design of spherically reconfigurable homogeneous modular soft robots," *Soft Robotics*, vol. 10, no. 1, pp. 52–65, 2023.

[6] B. T. Phillips, K. P. Becker, S. Kurumaya, K. C. Galloway, G. Whittredge, D. M. Vogt, C. B. Teeple, M. H. Rosen, V. A. Pieribone, D. F. Gruber, *et al.*, "A dexterous, glove-based teleoperable low-power soft robotic arm for delicate deep-sea biological exploration," *Scientific reports*, vol. 8, no. 1, pp. 1–9, 2018.

[7] Z. Jiao, C. Zhang, W. Wang, M. Pan, H. Yang, and J. Zou, "Advanced artificial muscle for flexible material-based reconfigurable soft robots," *Advanced Science*, vol. 6, no. 21, p. 1901371, 2019.

[8] F. Tao, H. Zhang, A. Liu, and A. Y. Nee, "Digital twin in industry: State-of-the-art," *IEEE Transactions on industrial informatics*, vol. 15, no. 4, pp. 2405–2415, 2018.

[9] Y. Cai, Y. Wang, and M. Burnett, "Using augmented reality to build digital twin for reconfigurable additive manufacturing system," *Journal of Manufacturing Systems*, vol. 56, pp. 598–604, 2020.

[10] C. Yang, S. Geng, I. Walker, D. T. Branson, J. Liu, J. S. Dai, and R. Kang, "Geometric constraint-based modeling and analysis of a novel continuum robot with shape memory alloy initiated variable stiffness," *The International Journal of Robotics Research*, vol. 39, no. 14, pp. 1620–1634, 2020.

[11] A. Koivikko, V. Lampinen, M. Pihlajamäki, K. Yiannacou, V. Sharma, and V. Sariola, "Integrated stretchable pneumatic strain gauges for electronics-free soft robots," *Communications Engineering*, vol. 1, no. 1, p. 14, 2022.

[12] S. Wang, Z. Sun, Y. Zhao, and L. Zuo, "A highly stretchable hydrogel sensor for soft robot multi-modal perception," *Sensors and Actuators A: Physical*, vol. 331, p. 113006, 2021.

[13] E. L. White, J. C. Case, and R. K. Kramer, "Multi-element strain gauge modules for soft sensory skins," *IEEE Sensors Journal*, vol. 16, no. 8, pp. 2607–2616, 2015.

[14] E. I. Borges, J. S. Rieder, D. Aschenbrenner, and R. B. Scharff, "Framework for armature-based 3d shape reconstruction of sensorized soft robots in extended reality," *Frontiers in Robotics and AI*, vol. 9, p. 810328, 2022.

[15] Z. Liao, J. Chen, and Y. Cai, "Reconfigurable soft robots based on modular design," *Computer-Aided Design & Applications*, 2023.

[16] Z. Liao, T. Li, Y. Wang, and Y. Cai, "Soft pneumatic actuator optimal design based on isogeometric analysis," *Manufacturing Letters*, vol. 35, pp. 55–63, 2023.

[17] J. S. Dai, "Euler–rodrigues formula variations, quaternion conjugation and intrinsic connections," *Mechanism and Machine Theory*, vol. 92, pp. 144–152, 2015.